Deformation and shape transitions in hot rotating neutron deficient Te isotopes

Mamta Aggarwal[1,2,*] and I. Mazumdar[2]

[1]*UM-DAE Centre for Excellence in Basic Sciences, University of Mumbai, Kalina Campus, Mumbai 400 098, India*

[2]*Tata Institute of Fundamental Research, Homi Bhabha Road, Colaba, Mumbai 400 005, India*

(Received 24 July 2008; revised manuscript received 11 May 2009; published 31 August 2009)

Evolution of the nuclear shapes and deformations under the influence of temperature and rotation is investigated in Te isotopes with neutron number ranging from the proton drip line to the stability valley. Spin dependent critical temperatures for the shape transitions in Te nuclei are computed. Shape transitions from prolate at low temperature and spin to oblate via triaxiality are seen with increasing neutron number and spin.

DOI: 10.1103/PhysRevC.80.024322 PACS number(s): 21.10.Dr, 27.60.+j, 21.60.−n

I. INTRODUCTION

The atomic nucleus undergoes a variety of shape transitions with increasing temperature and angular momentum. The study of such shape-phase transition such as phenomena in hot and rotating nuclei has established itself as a very active field of research in contemporary nuclear physics. Experimentally, a heavy-ion induced fusion reaction is one of the most potent tools to produce a compound nucleus at finite temperature and high angular momentum. The shape of the excited nuclei is best studied by analyzing the spectral shape and the angular anisotropy of the high energy gamma rays emitted from the decay of the giant dipole resonance (GDR) states [1,2]. Populating the compound nucleus at different initial excitation energies and carrying out exclusive measurement of the GDR gamma rays [3] from selected regions of temperature and angular momentum in the phase space, help us understand the shape evolution and phase transitions in hot-rotating nuclei.

On the theoretical front, various approaches have been used to study the shape transitions that can possibly take place at finite temperature and angular momentum. In general any theory of hot nuclei starts with a mean field approximation: the Hartree-Fock method [4] and Hartree-Fock-Bogoliubov theory [5], the Landau theory of shape transitions [6] developed by Alhassid and co-workers [7] where a large number of calculations are done for rare earth elements from cerium to hafnium [8]. The critical temperature of shape transitions extracted from these calculations is found to follow a systematic trend with the neutron number. An interesting finding in the calculations of the Hartree-Fock-Bogoliubov cranking formalism [9] by Goodman [10] has been a second critical temperature of the shape transition and the noncollective prolate phase of the nucleus bounded by the two spin dependent critical temperatures in the phase space [11,12]. A fully microscopic approach within the framework of the static path approximation (SPA) has also been introduced [13,14] recently which provides a general framework beyond the ordinary mean field approximation for studying the real time response function of a nucleus at a finite temperature.

We use a much simpler yet very effective theoretical formalism [15,16] to evaluate the nuclear shapes and deformations and study the structural transitions and their influence on the decay modes in the ground state and in the excited state nuclei. This formalism consists of the statistical theory of hot rotating nuclei [17,18] to treat the excited states of the nuclei which we blend with the well-known macroscopic-microscopic approach [19] proposed by Strutinsky [20] for the ground states of the nucleus in such a way that it reproduces the ground state shapes and deformations in good agreement with the available data and explains the structural transitions taking place and their influence on nucleon evaporation from the excited nuclei [21,22].

Recent developments in Radioactive Ion Beam facilities [23–26] have opened up the exciting possibilities to study nuclei near the drip lines and various experimental [25,27] and theoretical [28–31] works have revealed a lot of useful information about the drip-line nuclei [23,32] but the nuclear structure of drip-line nuclei under the influence of high angular momentum and temperature still needs attention. It is also required to calculate the movement of these nuclei on the phase space, i.e., the so-called shape-phase transitions and compare them with the experimental findings. The structural transitions also have influence on decay modes of the nuclei which we can understand through separation energy changes with temperature, rotation, and neutron number [15,22], therefore thorough study of structural transitions is a very important aspect of nuclear structure physics. Also, such theoretical calculations of shape transitions provide crucial insight in the planning of experiments and subsequent analysis of the shapes and shape fluctuations in hot-rotating nuclei. In this work, we find out the structural transitions in a host of Te isotopes from near the proton drip line to the stability valley as a function of temperature, rotation, and neutron number. We have calculated shape transitions for ^{103}Te to ^{124}Te scanning over a large range of temperature and angular momentum that can be probed by medium energy heavy ion facilities. In a subsequent paper we will be reporting similar calculations for very heavy nuclei around $A \approx 200$ [33] with a comparison with available experimental data [34,35].

There are two parts to the present approach:

(i) We suppress temperature and spin degree of freedom and evaluate ground state deformations and shape as a function of increasing neutron number for Te isotopes from $A = 103$ to 124 using a macroscopic-microscopic

*amamta@tifr.res.in

approach [19] by incorporating Strutinsky's shell correction [20] and deformation energy.

(ii) Effects of temperature and rotation on deformations and shape phase transitions in ^{105,108,116,122,124}Te isotopes are investigated using the statistical theory of hot rotating nuclei combined with macroscopic-microscopic approach [15].

II. THEORETICAL FORMALISM

We evaluate the ground state deformations and shapes within a macroscopic-microscopic approach in which the macroscopic binding energy $\mathrm{BE_{LDM}}$ is calculated using the mass formula of Moller-Nix [19] which is well suited to calculate binding energies over a wide range of nuclei. Microscopic effects arising due to a nonuniform distribution of nucleons are included through the Strutinsky's shell correction [20] to energy which is given as

$$\delta E = \sum_{i=1}^{A} \epsilon_i - \tilde{E}, \tag{1}$$

where the first term is the shell model energy in the ground state and the second term is the smoothed energy. The smearing width $\gamma \approx 1.2\hbar$ and levels up to $N = 11$ shells of the Nilsson model with Seegar parameters [36] are used. The single particle level schemes are different for protons and neutrons. The choice of these parameters makes the level scheme applicable over a wide range of mass numbers A. The diagonalization of the Hamiltonian is done with cylindrical basis states [37,38] with the Hill-Wheeler [39] deformation parameters (β, γ). The value of the angular deformation parameter γ ranges from -180° (oblate noncollective with symmetry axis parallel to rotation axis) to -120° (prolate collective with symmetry axis perpendicular to rotation axis) in steps of 10°. The axial deformation parameter β ranges from 0 to 0.4 in steps of 0.01.

When the shell correction δE is incorporated with the macroscopic binding energy of the spherical drop $\mathrm{BE_{LDM}}$ along with the deformation energy E_{def} gives the total corrected binding energy $\mathrm{BE_{cor}}$ which is maximized with respect to deformation parameters (β, γ) which give the deformation and shape of the ground state nucleus

$$\mathrm{BE_{cor}}(Z, N, \beta, \gamma) = \mathrm{BE_{LDM}}(Z, N) - E_{\mathrm{def}}(Z, N, \beta, \gamma) - \delta E(Z, N, \beta, \gamma). \tag{2}$$

The ground state one proton separation energy corrected for microscopic effects is obtained using the expression which helps trace the drip-line nuclei:

$$S_p^{\mathrm{cor}} = \mathrm{BE_{cor}}(Z, N, \beta, \gamma) - \mathrm{BE_{cor}}(Z-1, N, \beta, \gamma). \tag{3}$$

The excited and high spin states are treated by using the statistical theory which involves the determination of the grand partition function $Q(\alpha, \beta', \gamma')$ of the nuclear system of N neutrons and Z protons

$$Q(\alpha_Z, \alpha_N, \beta', \gamma') = \sum \exp(-\beta' E_i + \alpha_Z Z_i + \alpha_N N_i + \gamma' M_i), \tag{4}$$

where the Lagrangian multipliers α, β'[1], and γ'[1] conserve the particle number, total energy, and angular momentum of the system and are fixed by the saddle point equations. The conservation equations in terms of single-particle eigenvalues for the protons ϵ_i^Z with spin projection m_i^Z and neutrons ϵ_i^N with spin projection m_i^N [40], at a temperature $T(= 1/\beta')$ are

$$\langle Z \rangle = \sum n_i^Z = \sum \left[1 + \exp\left(-\alpha_Z + \beta' \epsilon_i - \gamma' m_i^Z\right)\right]^{-1}, \tag{5}$$

$$\langle N \rangle = \sum n_i^N = \sum \left[1 + \exp\left(-\alpha_N + \beta' \epsilon_i - \gamma' m_i^N\right)\right]^{-1}, \tag{6}$$

$$\langle E(M, T) \rangle = \sum n_i^Z \epsilon_i^Z + \sum n_i^N \epsilon_i^N, \tag{7}$$

$$\langle M \rangle = \sum n_i^Z m_i^Z + \sum n_i^N m_i^N, \tag{8}$$

where n_i is the occupation probability.

The excitation energy of the system is found by

$$E^*(M, T) = E(M, T) - E(0, 0), \tag{9}$$

where $E(0, 0)$ is the ground state energy of the nucleus given by

$$E(0, 0) = \sum \epsilon_i^Z + \sum \epsilon_i^N. \tag{10}$$

As illustrated by Moretto [41], the laboratory-fixed z axis can be made to coincide with the body-fixed z' axis and it is possible to identify and substitute M for the total angular momentum I. In the quantum-mechanical limit, the z component M of the total angular momentum $M = M_N + M_Z \to I + 1/2$, where I is the total angular momentum.

The rotational energy E_{rot} is calculated using Eq. (7):

$$E_{\mathrm{rot}}(M) = E(M, T) - E(0, T). \tag{11}$$

As $T \to 0$, E_{rot} corresponds to the yrast energy.

The entropy of the system is obtained by

$$S = -\sum [n_i ln n_i + (1 - n_i) ln(1 - n_i)]. \tag{12}$$

To evaluate the deformation and shape of the excited nucleus we calculate the excitation energy E^* and entropy S of the hot rotating nuclear system for fixed T and M as a function of β and γ and then incorporate them to the ground state energy corrected for microscopic effects and then minimize the free energy (F) with respect to deformation parameters (β, γ) at temperature T and angular momentum M

$$F(Z, N, T, M, \beta, \gamma) = E_{\mathrm{LDM}}(Z, N) + \delta E_{\mathrm{shell}}(\beta, \gamma) + E_{\mathrm{def}}(\beta, \gamma) + E^*(T, M, \beta, \gamma) - T S(T, M, \beta, \gamma). \tag{13}$$

[1]The Lagrangian multipliers β' and γ' should not be confused with the deformation parameters (β, γ). The primes are put just to differentiate them from deformation parameters. The notations β' and γ' used in the text from Eqs. (4) to (6) are Lagrangian multipliers, elsewhere in this article, β and γ are used as deformation parameters only.

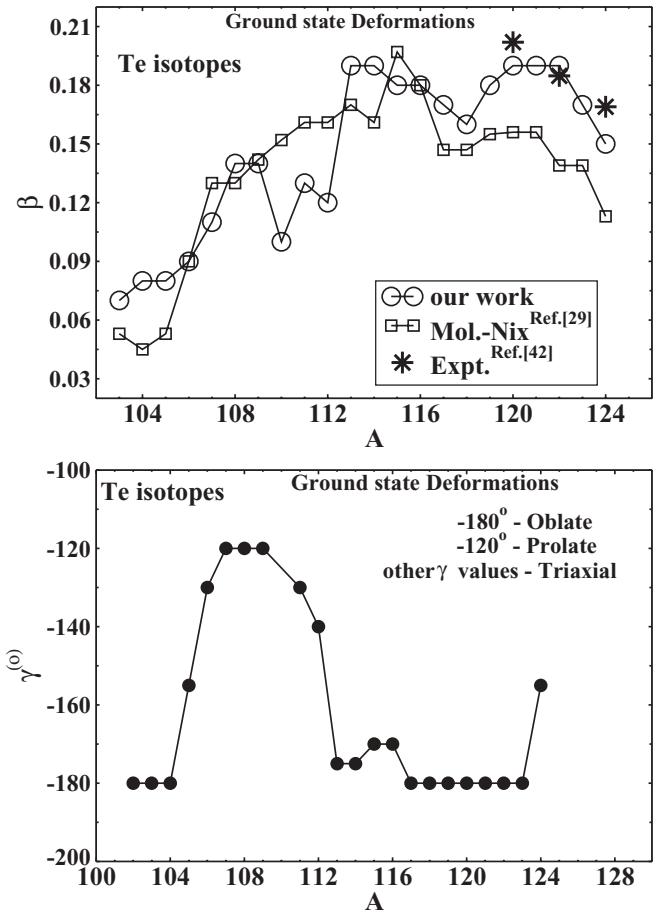

FIG. 1. (a) Equilibrium deformations parameter β vs. mass number A for $^{103-124}$Te in the ground state. (b) Equilibrium γ vs mass number for $^{103-124}$Te nuclei in the ground state.

The free energy minima gives the deformation and shape of the hot rotating nucleus.

III. RESULTS AND DISCUSSIONS

The ground state deformations calculated for $^{103-124}$Te nuclei are shown in Fig. 1(a). The agreement of our calculations with the available experimental [42] values for $A = 120, 122, 124$ is much better than the calculations of Moller and Nix [29]. Ground state shapes (γ) and deformations (β) show an interesting pattern with the neutron number. At $N = 51$, the nucleus is close to shell closure as well as the proton drip line. The deformation is very small near shell closure nuclei. As N increases from 51 (near closed shell) to 64 (midshell), the deformation (β) increases from 0.07 to 0.18. Around $N = 72$ ($\beta = 0.15$), the deformation has started decreasing slowly as it is again approaching the closed shell at $N = 82$. Among all the isotopes of Te studied here, the highest deformation is found in ^{113,114}Te with $\beta = 0.19$ and the least deformed nuclei are proton drip line nuclei $^{103-105}$Te lying near shell closure.

In the ground state, the shape changes with neutron number and it is more common for nuclear ground state shapes to be

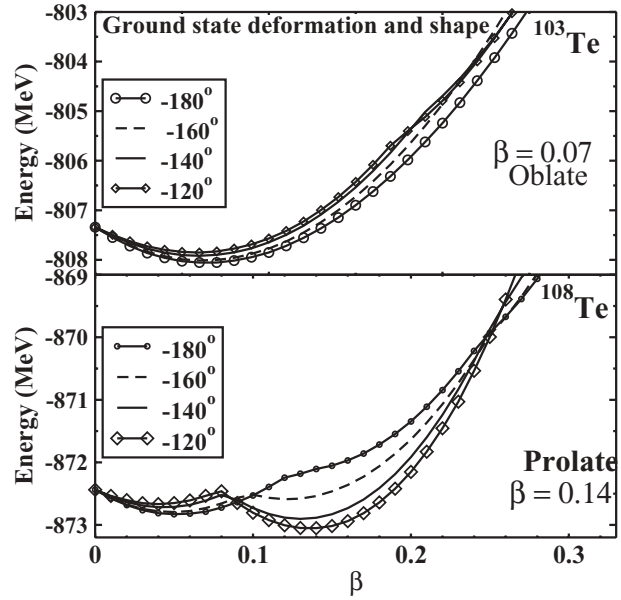

FIG. 2. Evaluation of the ground state shape and deformation of ^{103,108}Te by the minimization of energy with respect to deformation parameters β for different γ. The deformation and shape obtained is mentioned in the figure.

prolate than oblate though it is not true for all the nuclei. In the case of Te isotopes, we found that with the changing neutron number N, the nucleus goes through various interesting shape transitions in the ground state [see Fig. 1(b)]. Unstable nuclei ($N = 51, 52$) lying near the drip line have oblate shape ($\gamma = -180^\circ$) with very small deformation. The shape transition to triaxial shape at $N = 53$ (^{105}Te) to nearly prolate ($\gamma = -130^\circ$) at ^{106}Te and then to prolate ($\gamma = -120^\circ$) at ^{107}Te are seen. β is constantly increasing with N during all these shape transitions. The energy minimization giving us the shape and deformation of ^{103,108}Te in energy vs. β diagrams for different γ's is shown in Fig. 2. These simple curves provide us a very clear picture of the location of the minima at certain β, γ and also show the variation of energy at other β, γ. The shape transition to oblate ($\gamma = -180^\circ$) at $N = 65$ via triaxial at $N = 59$–63 takes place with changing N. The shape remains oblate up to $N = 71$. At $N = 72$, the shape again attains triaxial shape with declining deformation and finally approaches to sphericity at $N = 82$.

According to universally known features of the evolution of equilibrium shapes with temperature and spin, heating a deformed nonrotating nucleus leads to a shape transition from deformed to spherical at a certain temperature. At high temperatures $T \approx 2$ MeV, the shell effects melt and the nucleus resembles a classical liquid drop. The rotation of the hot nucleus generates an oblate shape rotating noncollectively. It has been shown by Goodman [43] that nuclei with two critical temperatures can rotate with a prolate shape about its symmetry axis. Such a phase exists in a narrow domain bound by the two spin dependent critical temperatures. Goodman has also shown that this rather unusual phase does not get washed out by shape fluctuations. Looking for such exotic shape-phase transitions has been one of our motivations in

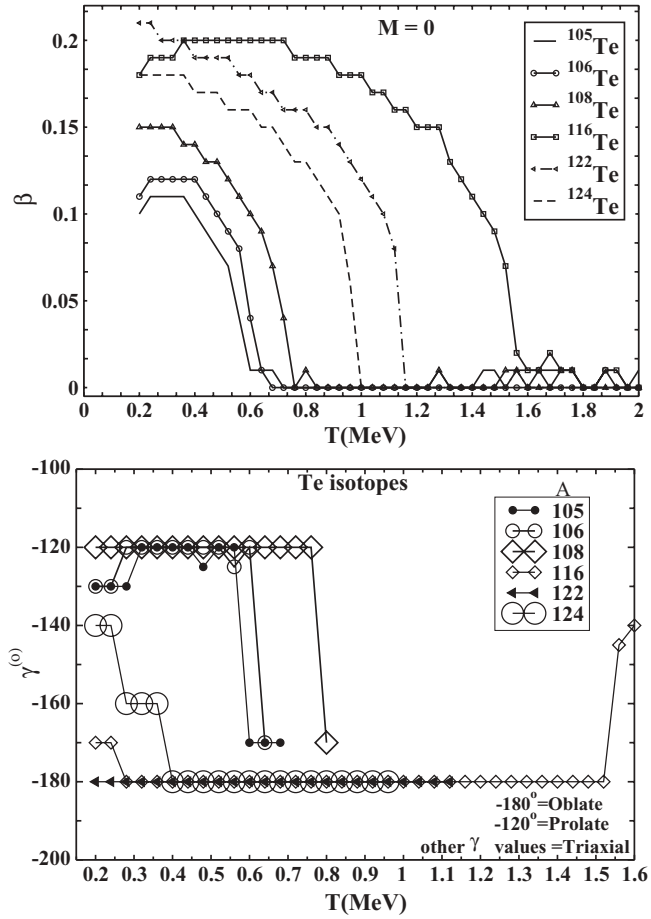

FIG. 3. (a) β vs. temperature T for ^{105,108,116,122,124}Te nuclei. (b) γ vs. temperature T for ^{105,108,116,122,124}Te nuclei.

our current program, in both PES calculations and GDR experiments [3,33–35]. We have seen such a behavior in our finite temperature PES calculations [33] for heavier nuclei, namely Au, Pt, and Hg. One of the authors has also observed such a behavior in ^{94}Ag in a very recent work [44]. With further rotation at higher T [45] and higher spin [44], the unexpected prolate noncollective phase undergoes the expected transition to oblate noncollective shape phase. However, no such phase has been seen in our present calculations for the Te isotopes. It is seen in the nuclei of certain mass regions only. The search for such rare shape-phase transitions still needs to be explored in much more detail.

We study deformation changes and shape-phase transitions as a function of temperature and angular momentum for ^{105,108,116,122,124}Te nuclei. Figures 3(a) and 3(b) show β and γ vs. temperature T, respectively, for ^{105,108,116,122,124}Te nuclei. As T increases, β decreases and approaches nearly 0 around $T = 1$ MeV in ^{105,108,124}Te nuclei whereas for ^{116}Te it takes higher T more than 1.5 MeV to reach zero deformation. Around $T = 2$ MeV, $\beta = 0$ for all Te isotopes studied here and the equilibrium shape is attaining sphericity. From Fig. 3(b), we note that the neutron deficient nuclei $^{105-108}$Te are prolate or nearly prolate at low T, suffer a shape transition to nearly oblate as T rises, and attain sphericity around $T \geqslant 1$ MeV but the neutron rich nucleus ^{122}Te is mostly oblate or nearly oblate at low T and remains oblate up to $T \approx 1$–1.1 MeV. The nucleus ^{116}Te which is the most deformed in ground as well as excited states remains deformed with oblate shape up to $T = 1.5$ MeV and attains sphericity at higher $T \approx 1.8$ MeV. The stable nucleus ^{124}Te is triaxial at low T, becomes oblate at $T = 0.4$ MeV, and remains so up to $T = 0.95$ MeV and then attains sphericity. Here we have plotted γ vs. T only for the deformed shape phase.

Figure 4 shows free energy minimization of the drip-line nucleus ^{105}Te with β and γ at fixed $T = 0.4$ MeV and those M values at which it faces shape transitions. ^{105}Te is slightly deformed ($\beta = 0.08$) in the ground state. When we incorporate the excitation energy, the initial prolate collective deformation ($\beta = 0.11$) at low T ($= 0.4$ MeV) [Fig. 4(a)] changes to oblate noncollective ($\beta = 0.10$) with cranking via triaxial shape at $M = 4\hbar$ [Fig. 4(b)] and then remains oblate at higher angular momentum. In Fig. 4(c) we note

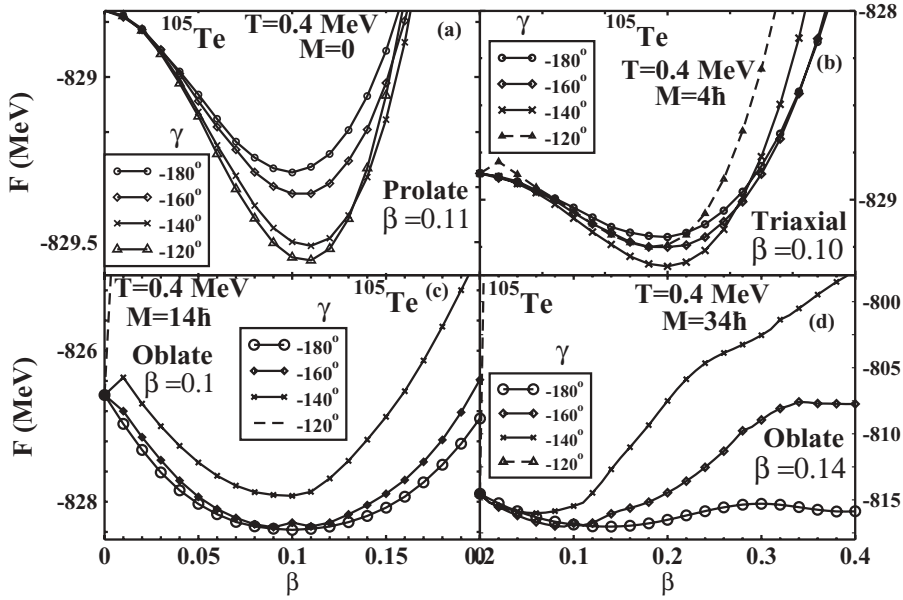

FIG. 4. Free energy minimization diagram showing F vs. β at various γ for ^{105}Te at $T = 0.4$ MeV and $M = 0$ (a), $4\hbar$ (b), $14\hbar$ (c), and $34\hbar$ (d). Shape and deformation corresponding to F minima are mentioned in each figure. We choose only those M values for this figure where some shape change or deformation jump is taking place.

that at $M = 14\hbar$, the shape is oblate noncollective but the triaxial shape with $\gamma = 160^\circ$ is also competing very closely for minima. However, the increasing angular momentum makes it reasonably well deformed with $\beta = 0.14$ with a well-defined minima at $34\hbar$ [Fig. 4(d)]. Increasing the temperature further up to 1 MeV starts reducing the deformation and drives the nucleus toward sphericity. The rotation of such a hot nucleus results in deformation with an oblate noncollective shape at $M = 4\hbar$ and remains the same at higher M values with larger β. Here it is to be noted that at low temperature the role of angular momentum is more prominent in taking the nucleus through various shape-phase transitions from prolate to triaxial and then to oblate with angular momentum changing from 0 to $14\hbar$, whereas at higher $T = 1$ MeV the shape is spherical at $M = 0$ and then the shape changes directly to oblate at $M = 4\hbar$ and remains so with gradually increasing M.

In the free energy vs. (β, γ) diagrams, different γ's compete very closely for free energy minima at low T and M, whereas at large T or M or both, the minima is very prominent for one value of γ and the corresponding shape is well defined and also the free energies corresponding to other γ's are very high comparatively. For example, at high oblate noncollective deformation at high M, the minima is clearly seen [Fig. 4(d)] whereas prolate collective ($\gamma = -120^\circ$) energies are very high which means that the probability for having a prolate collective shape is much less or negligible at those excitations energies. Similarly in Fig. 5(a), free energies corresponding to triaxial ($\gamma = -160^\circ$) and oblate ($\gamma = -180^\circ$) shape are very closely competing for minima whereas at high $T = 1.5$ MeV [Fig. 5(c)], the oblate shape minima is seen clearly and the free energy corresponding to the prolate shape ($\gamma = -120^\circ$) is very high as compared to those for $\gamma = -180^\circ$ which indicates that the possibility of the nucleus being prolate at that excitation is negligible. Figure 5 depicts the drive toward sphericity with increasing temperature at constant angular momentum $M = 10\hbar$ for ^{105}Te shown through the free energy minimization curve.

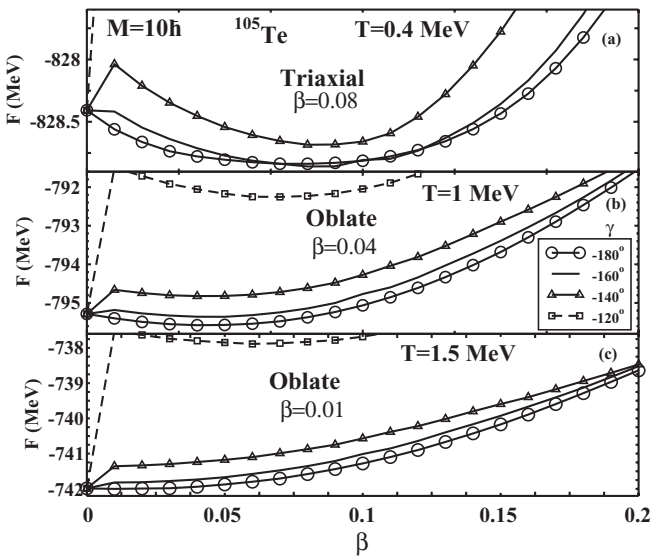

FIG. 5. Free energy minimization plot for rotating ^{105}Te at constant $M = 10\hbar$ with varying $T = 0.4$ MeV (a), 1.0 MeV (b), 1.5 MeV (c). Symbols for γ given in (b) are the same for (a) and (c).

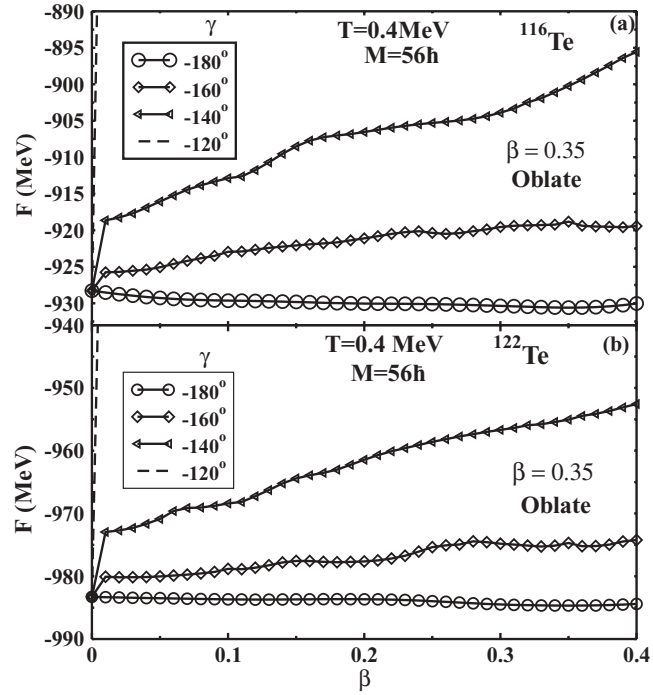

FIG. 6. F minima depicting the shape and deformation for (a)^{116}Te, (b) ^{122}Te at $T = 0.4$ MeV and $M = 56\hbar$.

Now moving toward the scenario for the stable isotope ^{122}Te we find that in the absence of rotation the large ground state deformation of $\beta = 0.2$ reaches near zero value beyond $T = 1$ MeV. However, with increasing angular momentum the

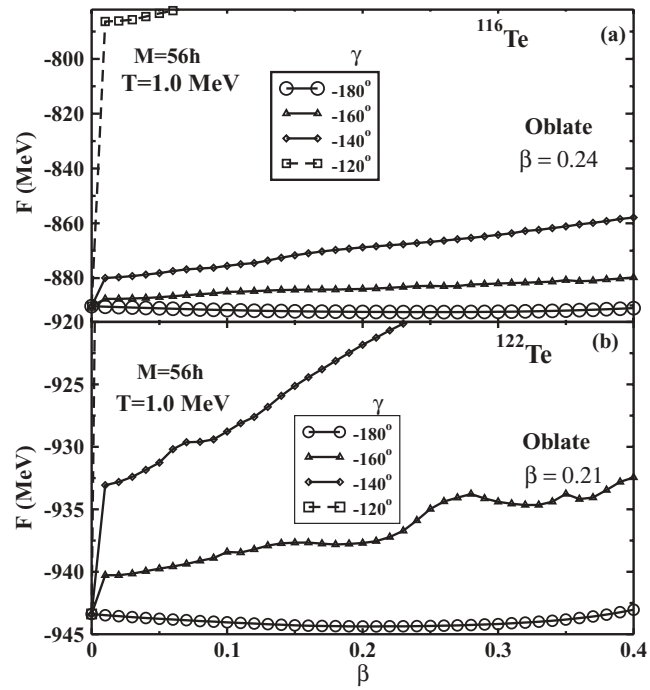

FIG. 7. F minima curves showing the shape and deformation for (a) ^{116}Te, (b) ^{122}Te at higher $T = 1.0$ MeV and $M = 56\hbar$.

hot nuclear system gets deformed and is oblate with a large deformation of $\beta = 0.21$ at $M = 56\hbar$ even at temperature $T = 1$ MeV. At lower temperature $T = 0.4$ MeV, it has a very large deformation $\beta = 0.35$ at $M = 56\hbar$. The largest deformation seen in the Te isotopes studied in this work is $\beta = 0.36$ for ^{122}Te at $T = 0.4$ MeV and $M = 60\hbar$. Figure 6 shows these large deformations attained by the rotating nuclear systems at high angular momentum value $M = 56\hbar$ in ^{116,122}Te at low $T = 0.4$ MeV. With such rotation, these nuclear systems remain highly deformed even at high temperature $T = 1$ MeV (see Fig. 7).

As the nucleus is an ensemble of a finite number of particles it is expected to experience shape fluctuations. The deformations of a minimum free energy that we calculate are the so-called most probable or mean field deformations and may be different from the average deformation which is why it is required to calculate the average shape. However, at low temperatures, shape fluctuations are small and the average shape is similar to the most probable shape. Fluctuations start smoothing out the sharp transitions at higher temperatures. The effect of shape fluctuations and detailed discussions for these Te isotopes will be presented in a forthcoming article [33].

IV. CONCLUSION

A systematic study of structural effects with a simple theoretical formalism has been presented which provided us with very useful results for ground as well as excited states of Te isotopes. We have computed ground state shapes and deformations for Te isotopes from $A = 103$ to 124 covering a wide region from near the drip line to the valley of stability. We have found a systematic pattern in the change in deformation and shape with increasing neutron number. Proton rich Te nuclei are less deformed with prolate collective or nearly prolate shapes than those near the stability valley which are well deformed with oblate noncollective shape. Incorporating excitations through statistical theory, the shape transitions for hot rotating ^{105,108,116,122,124}Te nuclei have been calculated from $T = 0$ to 2 MeV and $M = 0$ to $60\hbar$. The Te isotopes are found to have gone through a variety of shape transitions which are shown through the free energy minimization curves with respect to deformation parameters β and γ.

The critical temperatures for these Te isotopes at which the ground state deformation vanishes to zero for zero angular momentum are calculated. It is found that while increasing temperature at constant or no angular momentum drives the system toward spherical shape, the increase in angular momentum tries to make it more deformed with oblate shape at constant temperatures. At high angular momentum, the shape is oblate but the deformation is quite high even at high temperature. Proton rich nuclei ^{105,108}Te are also well deformed in an excited high angular momentum state though they were only slightly deformed in the ground state. These nuclei go through all shapes from prolate to triaxial to oblate with varied deformations whereas at high N and M the shape is oblate noncollective only with large deformation. It will be interesting to compare these calculations with experimental predictions obtained from the study of GDR decay gamma rays from these isotopes. The role of thermal and orientation fluctuations at finite temperature and spin will try to smoothen out the equilibrium deformations obtained from our basic calculations. The effect of fluctuation will be discussed in a future publication. The calculations for very heavy systems for $A \approx 200$ will also be discussed in a subsequent publication along with a comparison with experimental data from GDR decay studies.

ACKNOWLEDGMENTS

M.A. thanks financial support from CSIR and Department of Science and Technology (DST), New Delhi, India.

[1] J. O. Newton, B. Herskind, R. M. Diamond, E. L. Dines, J. E. Draper, K. H. Lindenberger, C. Schuck, S. Shih, and F. S. Stephens, Phys. Rev. Lett. **46**, 1383 (1981).
[2] K. A. Snover, Annu. Rev. Nucl. Part. Sci. **36**, 545 (1986); **42**, 483 (1992).
[3] I. Mazumdar, Y. K. Agarwal, D. A. Gothe, and U. Kadhane, Nucl. Phys. **A731**, 146 (2004).
[4] J. Bartel and P. Quentin, Phys. Lett. **B152**, 29 (1985).
[5] P. Quentin and H. Flocard, Annu. Rev. Nucl. Part. Sci. **28**, 523 (1978).
[6] S. Levit and Y. Alhassid, Nucl. Phys. **A413**, 439 (1984).
[7] Y. Alhassid, S. Levit, and J. Zingman, Phys. Rev. Lett. **57**, 539 (1986).
[8] Y. Alhassid, J. M. Manoyan, and S. Levit, Phys. Rev. Lett. **63**, 31 (1989).
[9] A. L. Goodman, Nucl. Phys. **A352**, 30 (1981).
[10] A. L. Goodman, Phys. Rev. C **39**, 2008 (1989), and references therein.
[11] A. L. Goodman, Phys. Rev. Lett. **73**, 416 (1994).
[12] A. L. Goodman, Nucl. Phys. **A591**, 182 (1995).
[13] B. K. Agrawal and A. Ansari, Nucl. Phys. **A567**, 1 (1994).
[14] R. Rossignoli, N. Canosa, and J. L. Egido, Nucl. Phys. **A607**, 250 (1996).
[15] Mamta Aggarwal, Phys. Rev. C **69**, 034602 (2004).
[16] M. Rajasekaran and Mamta Aggarwal, Int. J. Mod. Phys. E **7**, 389 (1998).
[17] M. Rajasekaran, T. R. Rajasekaran, and N. Arunachalam, Phys. Rev. C **37**, 307 (1988).
[18] M. Rajasekaran, N. Arunachalam, and V. Devanathan, Phys. Rev. C **36**, 1860 (1987).
[19] P. Moller, J. R. Nix, W. D. Myers, and W. J. Swiatecki, At. Data Nucl. Data Tables **59**, 185 (1995).
[20] V. M. Strutinsky, Nucl. Phys. **A95**, 420 (1967).
[21] M. Rajasekaran and Mamta Aggarwal, Phys. Rev. C **58**, 2743 (1998).
[22] Mamta Aggarwal, Int. J. Mod. Phys. E **17**, 1091 (2008).
[23] C. Detraz *et al.*, Nucl. Phys. **A519**, 529 (1990).
[24] V. Borrel *et al.*, Z. Phys. A **344**, 135 (1992); R. J. Irvine *et al.*, Phys. Rev. C **55**, R1621 (1997).
[25] M. F. Mohar, D. Bazin, W. Benenson, D. J. Morrissey, N. A. Orr, B. M. Sherrill, D. Swan, J. A. Winger, A. C. Mueller, and D. Guillemaud-Mueller, Phys. Rev. Lett. **66**, 1571 (1991).

[26] J. A. Winger *et al.*, Phys. Lett. **B299**, 214 (1993).
[27] F. Pougheon *et al.*, Z. Phys. A **327**, 17 (1987).
[28] W. E. Ormand, Phys. Rev. C **55**, 2407 (1997).
[29] P. Moller and J. R. Nix, At. Data Nucl. Data Tables **66**, 131 (1997).
[30] R. Smolanczuk and J. Dobaczewski, Phys. Rev. C **48**, R2166 (1993).
[31] G. A. Lalazissis and S. Raman, Phys. Rev. C **58**, 1467 (1998).
[32] K. Riisager, Rev. Mod. Phys. **66**, 1105 (1994).
[33] Mamta Aggarwal and I. Mazumdar (under preparation).
[34] I. Mazumdar, D. A. Gothe, G. Anil Kumar, M. Aggarwal, P. K. Joshi, R. Palit, and H. C. Jain, Acta Phys. Pol. B **40**, 545 (2009).
[35] I. Mazumdar, H. C. Jain, R. Palit, D. A. Gothe, P. K. Joshi, and M. Aggarwal, Acta Phys. Pol. B **38**, 1463 (2007).
[36] P. A. Seeger, Nucl. Phys. **A238**, 491 (1975).
[37] J. M. Eisenberg and W. Greiner, *Microscopic Theory of Nucleus* (North Holland, New York, 1976).
[38] G. Shanmugam, P. R. Subramanian, M. Rajasekaran, and V. Devanathan, *Nuclear Interactions*, Lecture Notes in Physics, Vol. 72 (Springer, Berlin, 1979), p. 433.
[39] D. L. Hill and J. A. Wheeler, Phys. Rev. **89**, 1102 (1953).
[40] J. B. Huizenga and L. G. Moretto, Annu. Rev. Nucl. Sci. **22**, 427 (1972).
[41] L. G. Moretto, Nucl. Phys. **A182**, 641 (1972); **A185**, 145 (1972); **A216**, 1 (1973).
[42] S. Raman *et al.*, At. Data Nucl. Data Tables **36**, 1 (1987).
[43] A. L. Goodman, Phys. Rev. Lett. **73**, 416 (1994).
[44] Mamta Aggarwal, Phys. Lett. B (communicated).
[45] A. L. Goodman and Tanihao Jin, Nucl. Phys. **A611**, 139 (1996).